POWER-LAW TAILS OF THE DENSITY DISTRIBUTION IN STAR-FORMING CLOUDS: POSSIBLE EFFECTS OF ROTATION AND THERMODYNAMICS

Todor Veltchev[1], Lyubov Marinkova[2], Sava Donkov[3] & Orlin Stanchev[1]

[1] Faculty of Physics, University of Sofia, 5 James Bourchier Blvd., 1164 Sofia, Bulgaria

[2] Department of Applied Physics, Technical University-Sofia, 8 Kliment Ohridski Blvd., Sofia 1000, Bulgaria

[3] Institute of Astronomy and NAO, Bulgarian Academy of Sciences, 72 Tsarigradsko Chausee Blvd., 1784 Sofia, Bulgaria

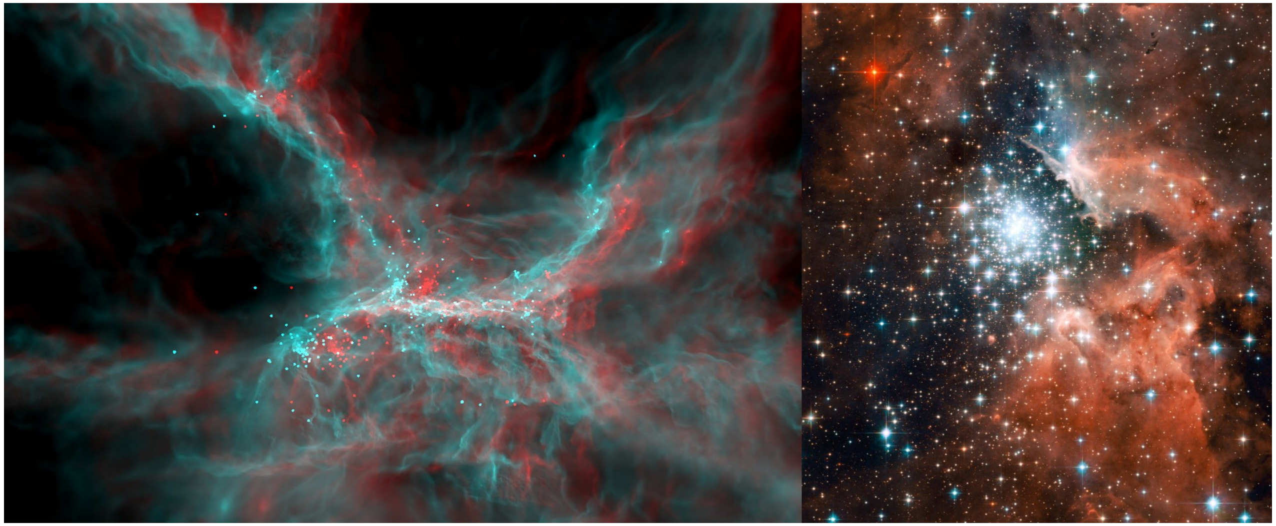

XIIIth Bulgarian-Serbian Astronomical Conference
3-7 October 2022, Velingrad, Bulgaiia

Molecular clouds (MCs) as sites of star formation (SF)

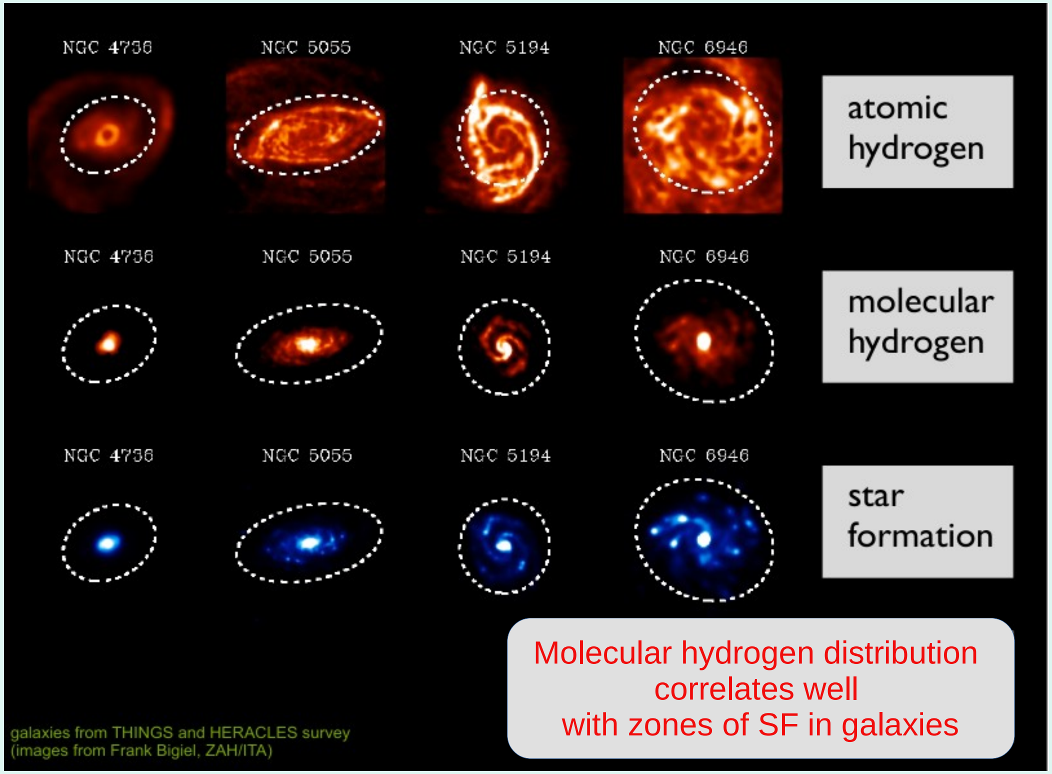

galaxies from THINGS and HERACLES survey
(images from Frank Bigiel, ZAH/ITA)

Molecular hydrogen distribution
correlates well
with zones of SF in galaxies

Molecular clouds (MCs) as sites of star formation (SF)

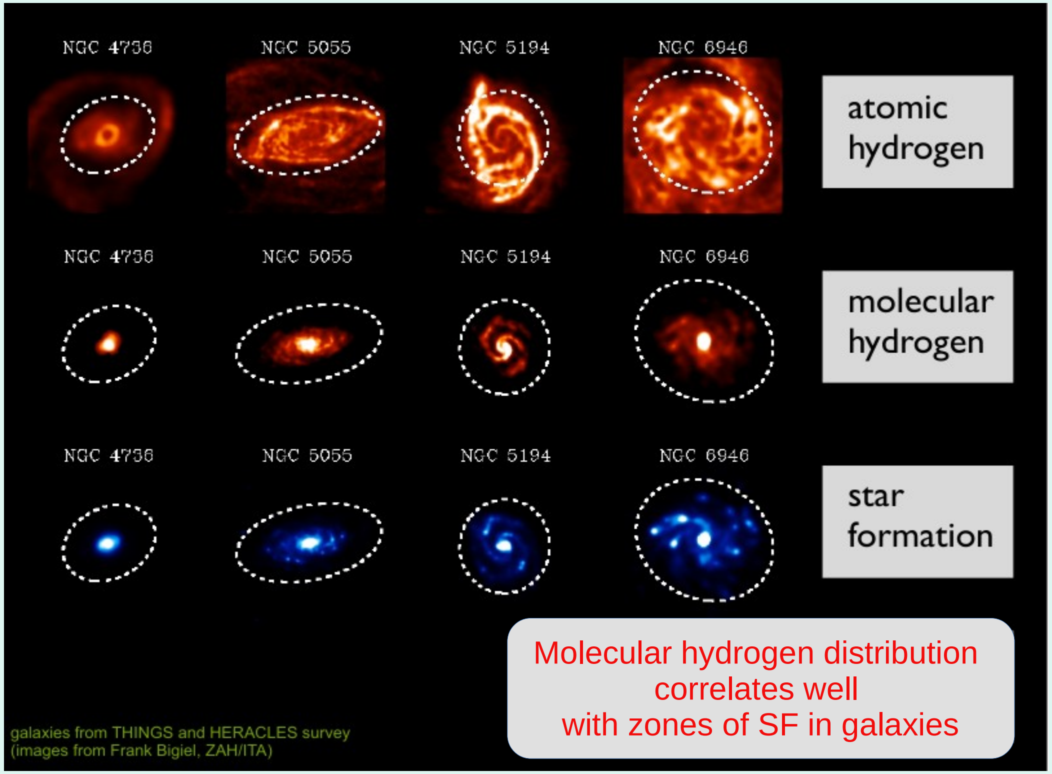

Molecular hydrogen distribution correlates well with zones of SF in galaxies

galaxies from THINGS and HERACLES survey
(images from Frank Bigiel, ZAH/ITA)

Tracers of molecular gas

Dust extinction
('dark clouds')

MC ρ Ophiuchi
(image: HST, DSS1; sky.esa.int)

Molecular clouds (MCs) as sites of star formation (SF)

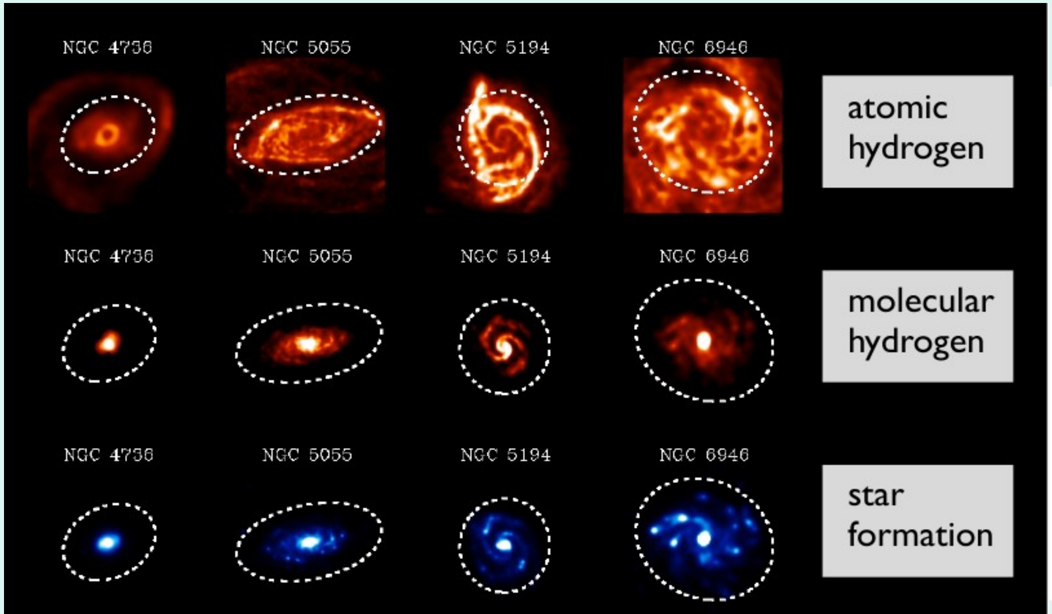

Molecular hydrogen distribution correlates well
with zones of SF in galaxies

galaxies from THINGS and HERACLES survey
(images from Frank Bigiel, ZAH/ITA)

Tracers of molecular gas

Emission of CO species

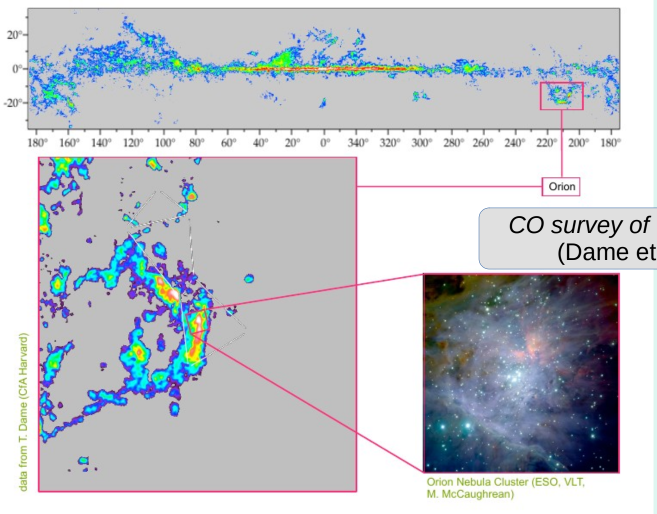

CO survey of the Milky Way
(Dame et al. 2001)

Dust extinction
(‘dark clouds’)

MC ρ Ophiuchi
(image: HST, DSS1; sky.esa.int)

Molecular clouds (MCs) as sites of star formation (SF)

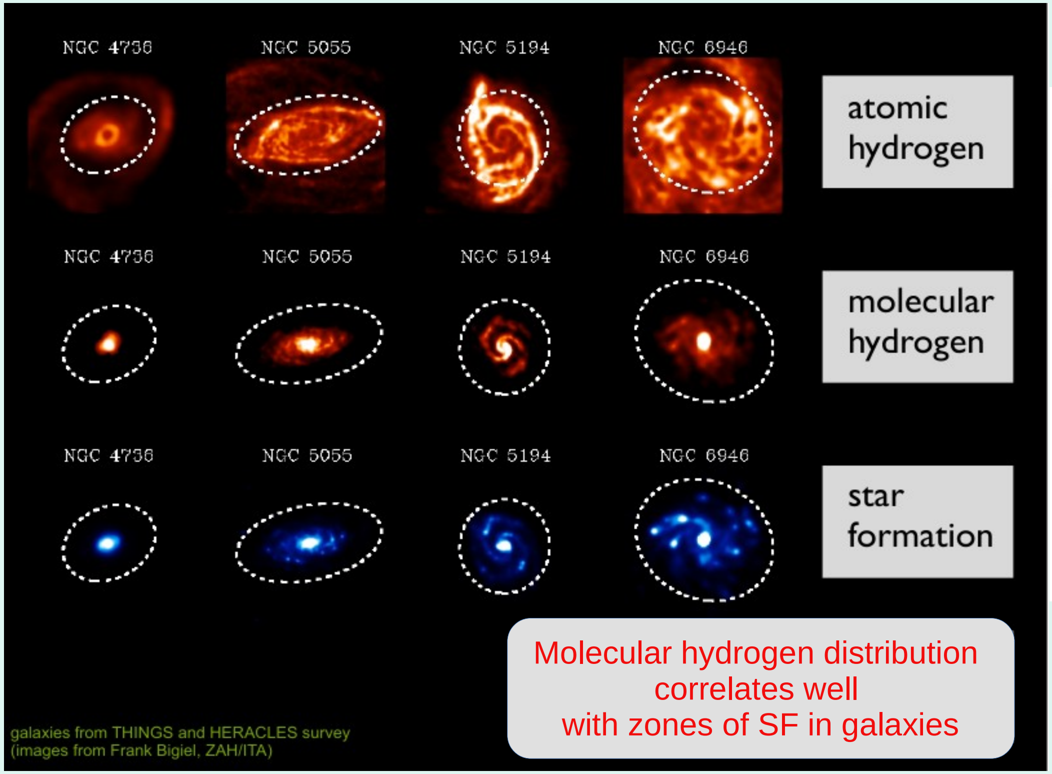

Molecular hydrogen distribution correlates well with zones of SF in galaxies

galaxies from THINGS and HERACLES survey
(images from Frank Bigiel, ZAH/ITA)

Tracers of molecular gas

Emission of CO species

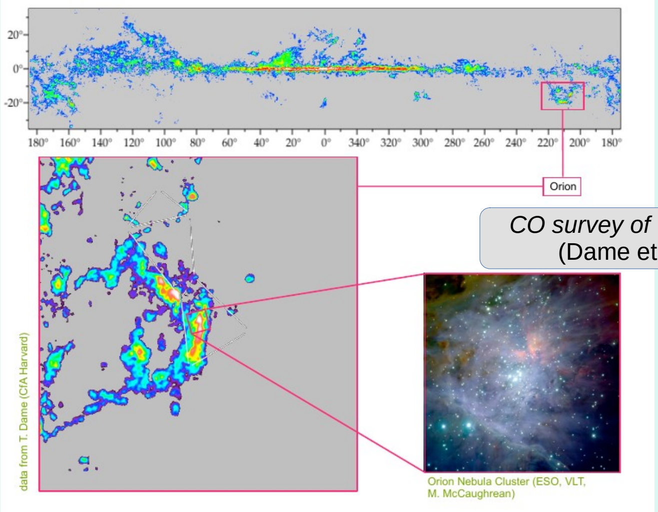

Orion Nebula Cluster (ESO, VLT, M. McCaughrean)

CO survey of the Milky Way
(Dame et al. 2001)

Dust emission
(small-scale structure)

MC ρ Ophiuchi
(image: Herschel SPIRE 250, 350, 500 µm)

Dust extinction
('dark clouds')

MC ρ Ophiuchi
(image: HST, DSS1; sky.esa.int)

Appropriate
for study of star-forming
clouds and their
substructures (e.g.,
pre-/protostellar cores)

The variety of star-forming activity in molecular clouds (MCs)

Herschel imaging at high angular resolution (18 arcsec; Schneider et al. 2022)

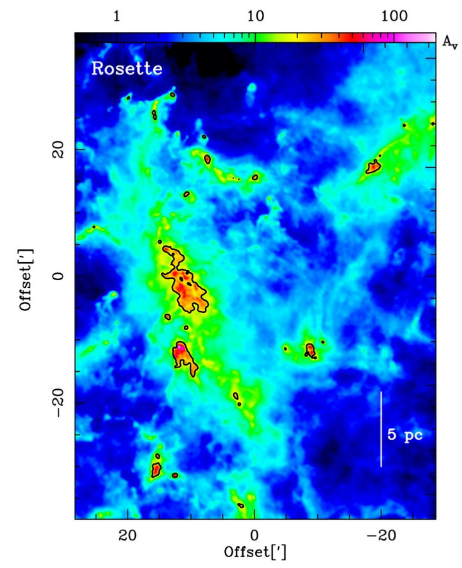

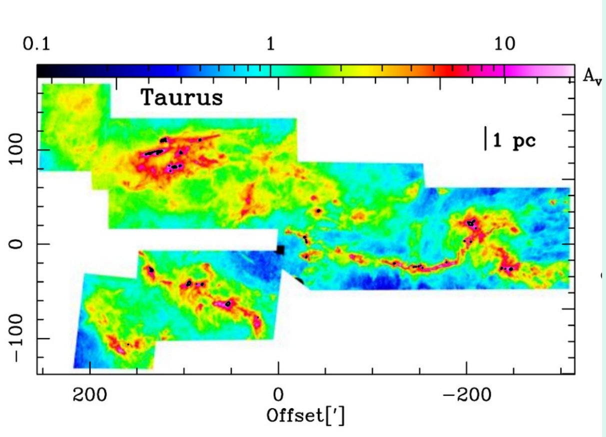

High-mass SF clouds

- giant MCs
- sizes: up to 100 pc
- masses: 10^5-10^6 $M_\odot$
- Signatures of high-mass and cluster formation, massive, grav. unstable filaments of high column-density

Low-mass SF clouds

- sizes: up to 10-30 pc
- masses: 10^3-10^4 $M_\odot$
- They form typically low-mass stars

The variety of star-forming activity in molecular clouds (MCs)

Herschel imaging at high angular resolution (18 arcsec; Schneider et al. 2022)

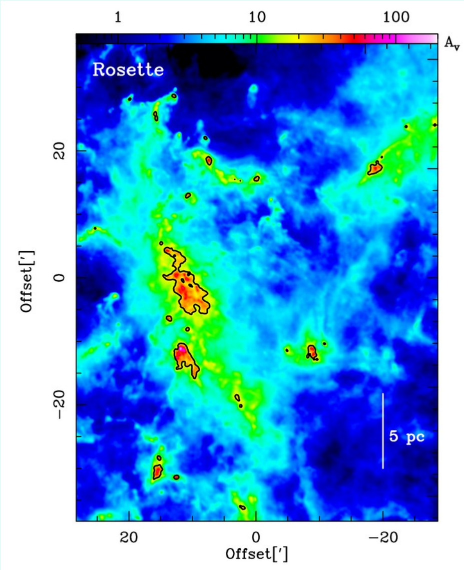

High-mass SF clouds

- giant MCs
- sizes: up to 100 pc
- masses: 10^5-10^6 $M_\odot$
- Signatures of high-mass and cluster formation, massive, grav. unstable filaments of high column-density

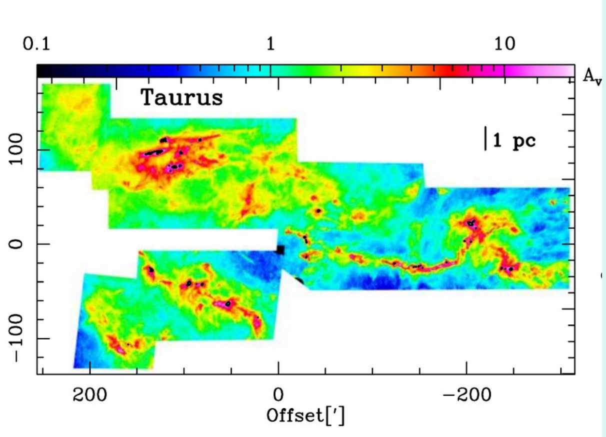

Low-mass SF clouds

- sizes: up to 10-30 pc
- masses: 10^3-10^4 $M_\odot$
- They form typically low-mass stars

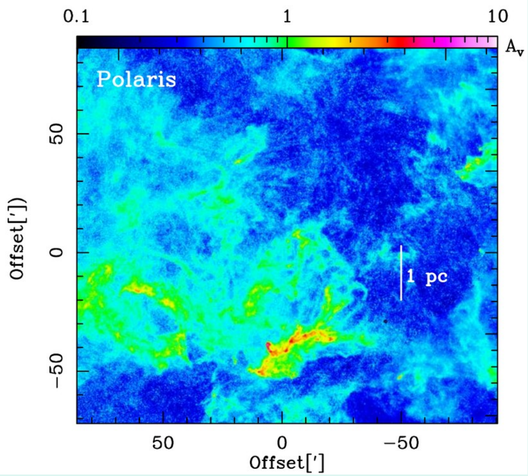

Quiescent clouds

- Poor or no SF activity

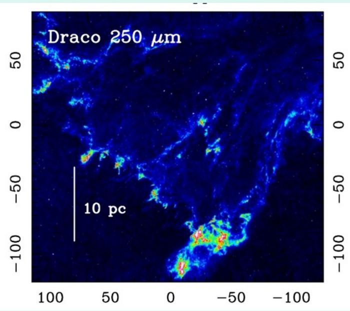

Diffuse clouds

- Mostly atomic

The complex physics of star-forming MCs

- The complex physics of MCs is governed by gravity, supersonic turbulence, magnetic fields and – in the general case – an isothermal equation of state (EOS).
- Accretion from the surrounding medium and feedback from new-born stars and supernovae play an essential role in cloud’s evolution.
- Effects of rotation

The complex physics of star-forming MCs

- The complex physics of MCs is governed by gravity, supersonic turbulence, magnetic fields and – in the general case – an isothermal equation of state (EOS).
- Accretion from the surrounding medium and feedback from new-born stars and supernovae play an essential role in cloud’s evolution.
- Effects of rotation

This complex physics is imprinted in:

- General structure of MCs in terms of scaling relations of velocity dispersion and mass.
- Probability distribution of different quantities of the medium
- Physical parameters of substructures (clumps, cores, filaments)

(Column-)Density distribution as a research tool

$s = \log(\rho/\langle\rho\rangle)$ $p_s \mathrm{d}s$ - probability distribution function (PDF) of logdensity

Lognormal (part of) PDF
→ isothermal supersonic turbulence

$$p_s \mathrm{d}s = \frac{1}{\sqrt{2\pi\sigma_s^2}} \exp\left[-\frac{(s-s_0)^2}{2\sigma_s^2}\right] \mathrm{d}s \qquad \sigma_s^2 = \ln\left[1 + b^2 \mathcal{M}^2\right]$$

simulations

observations

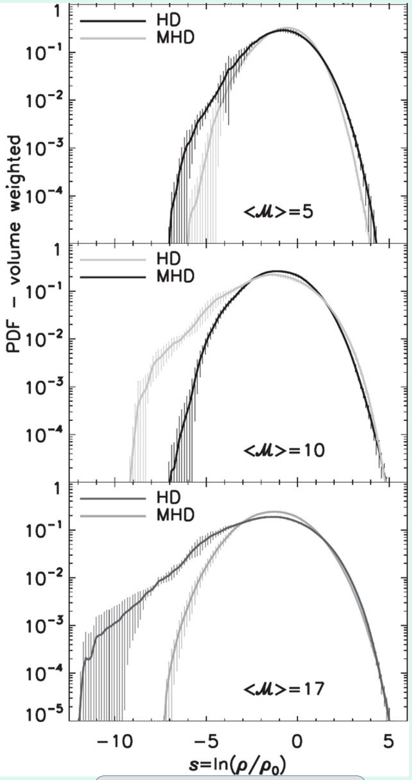

Molina et al. (2012)

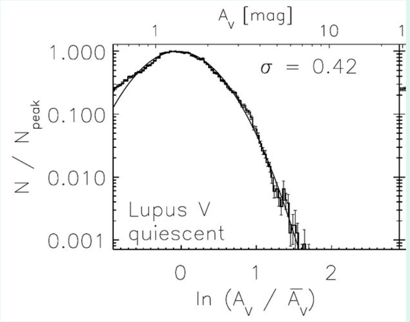

Kainulainen et al. (2009)

(Column-)Density distribution as a research tool

$s = \log(\rho/\langle\rho\rangle)$ $p_s \mathrm{d}s$ - probability distribution function (PDF) of logdensity

Lognormal (part of) PDF → isothermal supersonic turbulence

$$p_s \mathrm{d}s = \frac{1}{\sqrt{2\pi\sigma_s^2}} \exp\left[-\frac{(s-s_0)^2}{2\sigma_s^2}\right] \mathrm{d}s \qquad \sigma_s^2 = \ln\left[1 + b^2\mathcal{M}^2\right]$$

simulations

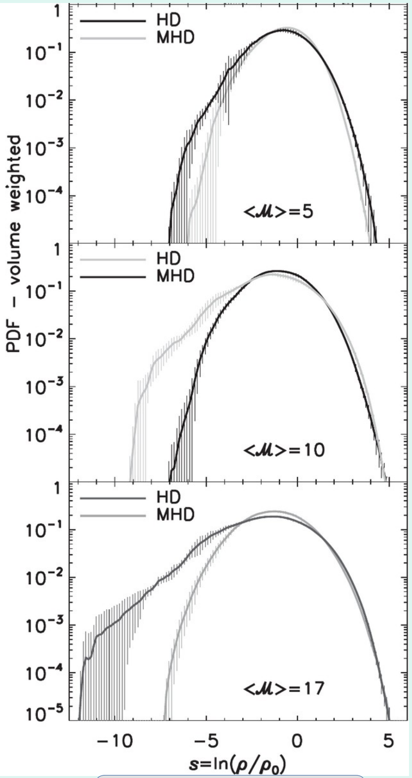

Molina et al. (2012)

observations

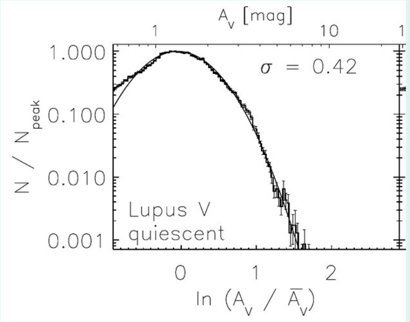

Kainulainen et al. (2009)

Emergence of a power-law tail (PLT) → increasing role of self-gravity

$$\mathrm{PLT} \propto \exp(qs)\,, \quad q < 0$$

simulations

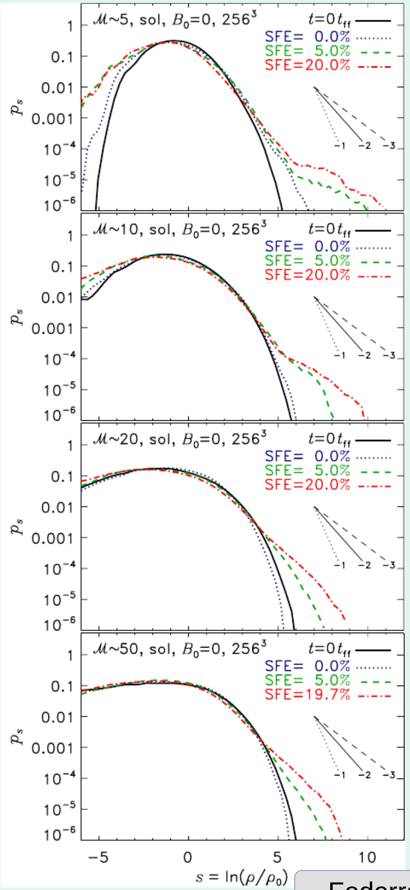

Federrath & Klessen (2013)

observations

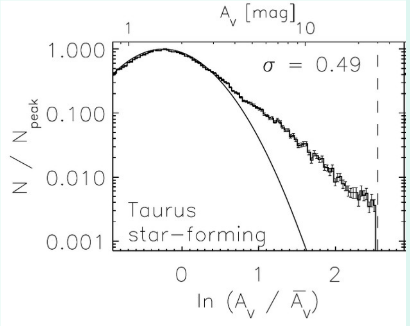

Kainulainen et al. (2009)

PDF of mass density (ρ-PDF) in evolved star-forming MCs

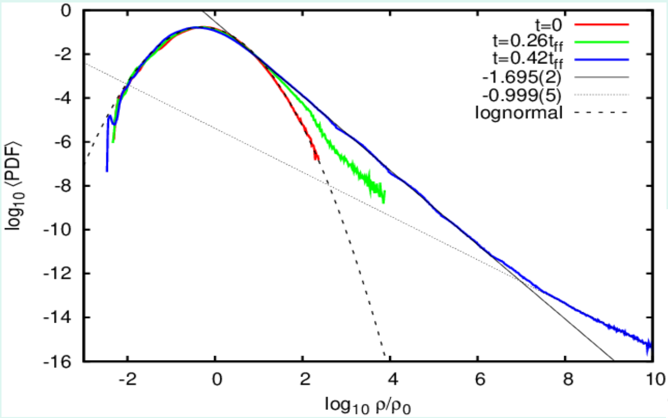

Kritsuk, Norman & Wagner (2011)

- HD simulations of supersonic, isothermal and self-gravitating turbulent medium.
- Resolution: down to AU scales in the dense cores.

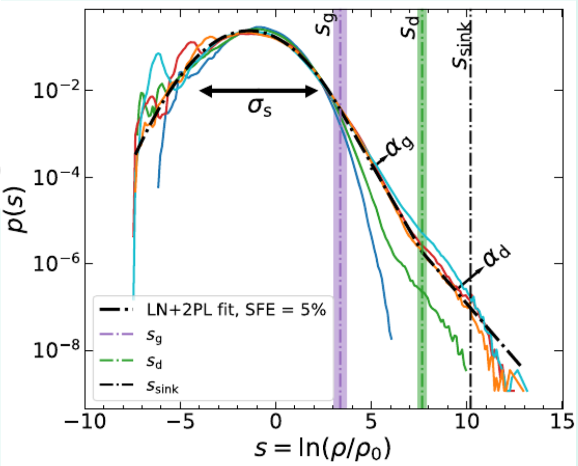

Khullar et al. (2021)

- HD simulations of isothermal gravoturbulent fluids, varying the virial ratio and the Mach number.
- Resolution: down to ~100 AU.

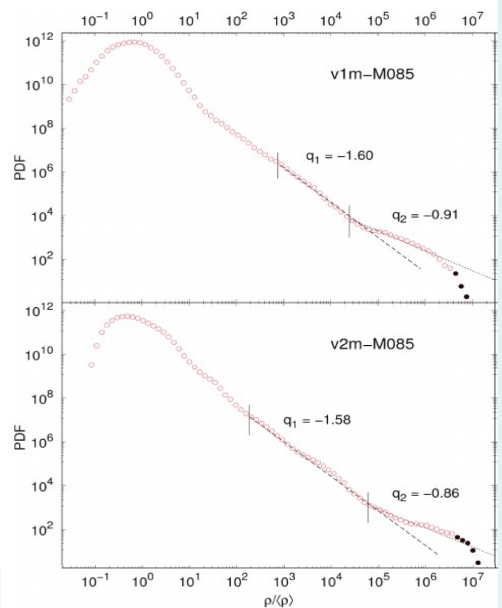

Marinkova et al. (2021)

- HD simulations of typical large SF clumps (0.5 pc), with large Jeans content (32, 354 M_J); variation of turbulent driving
- Resolution: down to ~3 AU.

PDF of mass density (*ρ*-PDF) in evolved star-forming MCs

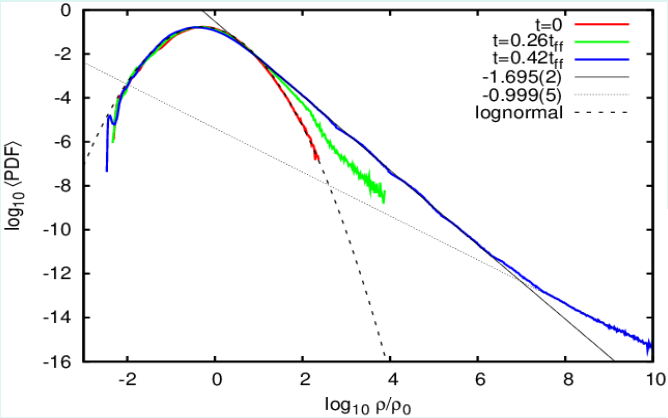

Kritsuk, Norman & Wagner (2011)

- HD simulations of supersonic, isothermal and self-gravitating turbulent medium.
- Resolution: down to AU scales in the dense cores.

Emergence of a ***second*** *PLT at very high densities and at later evolutionary stages*

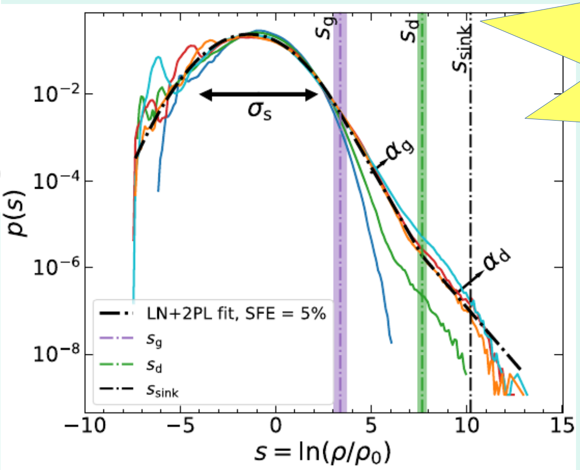

Khullar et al. (2021)

- HD simulations of isothermal gravoturbulent fluids, varying the virial ratio and the Mach number.
- Resolution: down to ~100 AU.

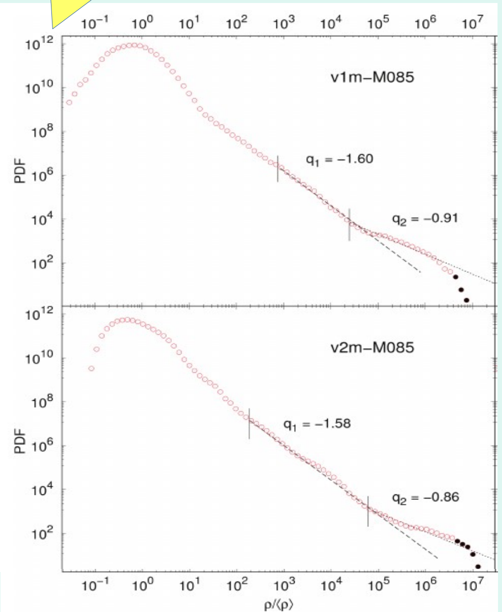

Marinkova et al. (2021)

- HD simulations of typical large SF clumps (0.5 pc), with large Jeans content (32, 354 M_J); variation of turbulent driving
- Resolution: down to ~3 AU.

N-PDFs of variety of MCs with various SF activity

Herschel imaging at high angular resolution (18 arcsec; Schneider et al. 2022)

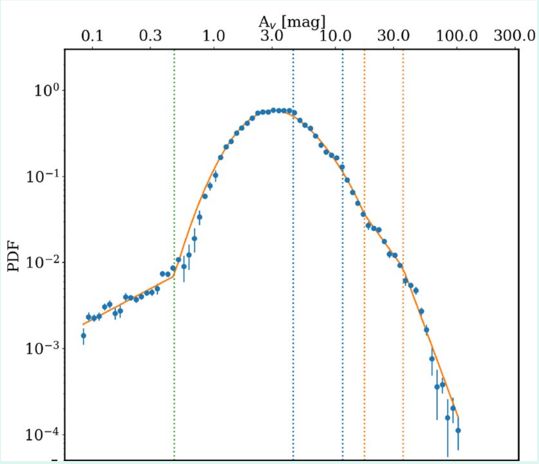

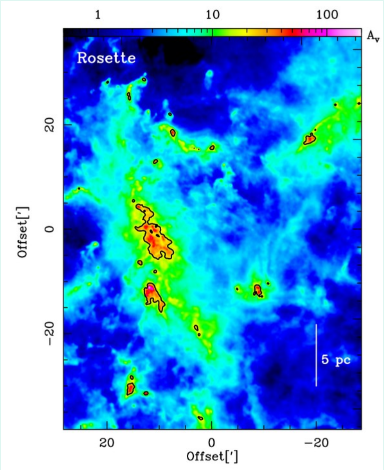

High-mass SF clouds

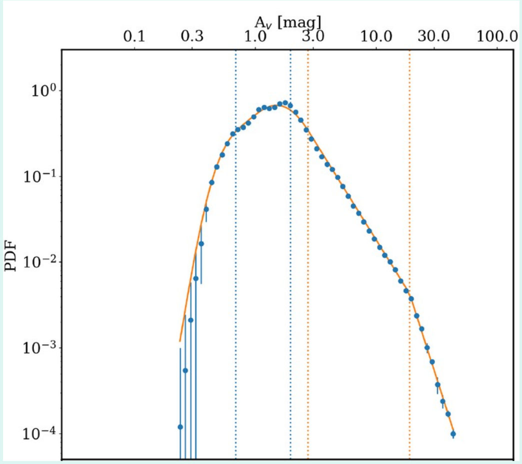

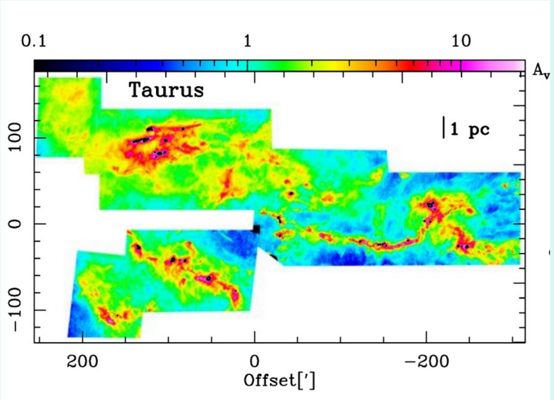

Low-mass SF clouds

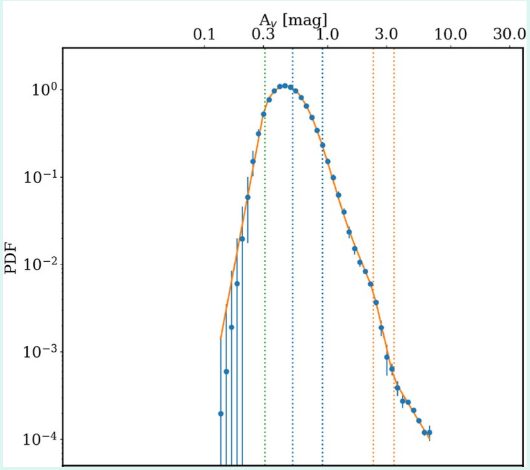

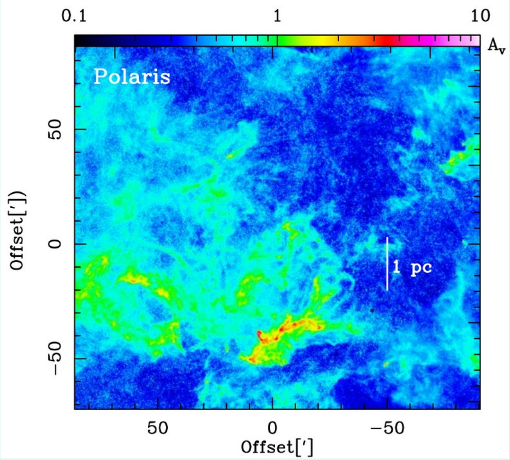

Quiescent clouds

N-PDFs of variety of MCs with various SF activity

Herschel imaging at high angular resolution (18 arcsec; Schneider et al. 2022)

*Double PLTs **confirmed** from observations!*

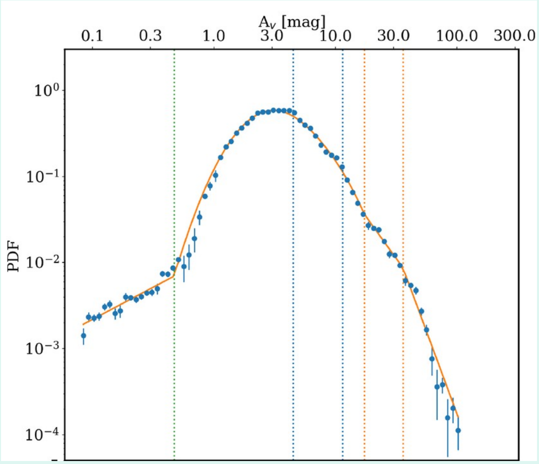

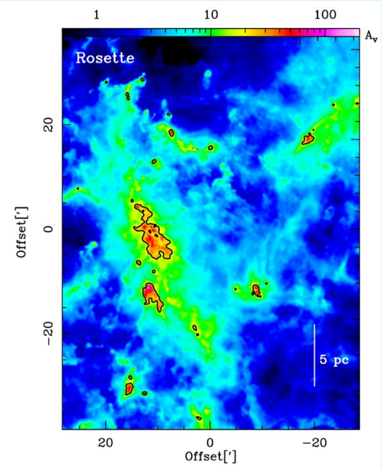

High-mass SF clouds

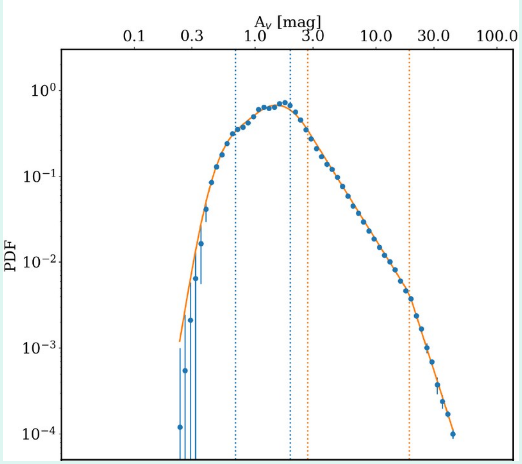

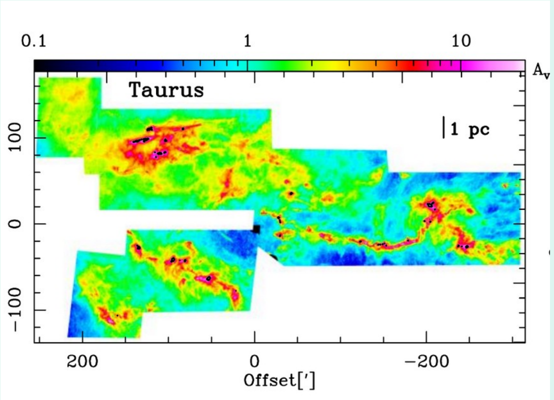

Low-mass SF clouds

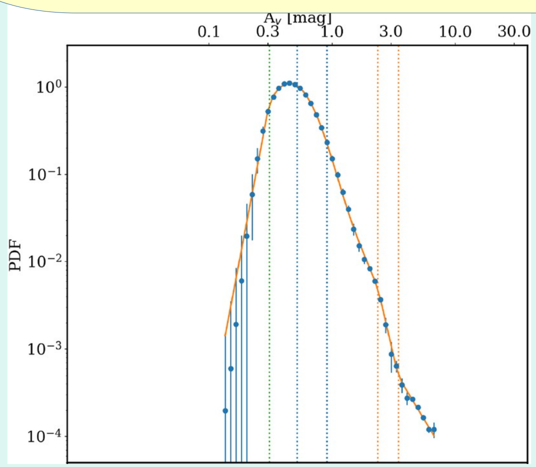

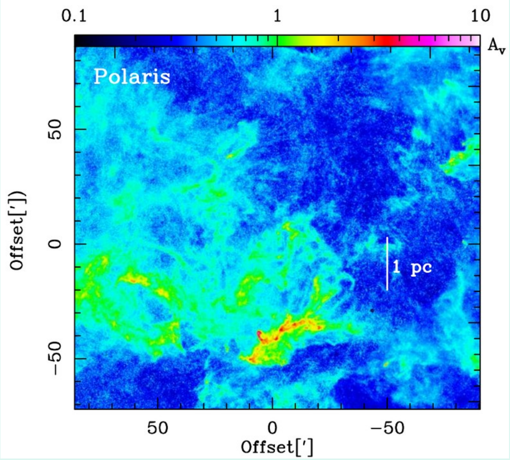

Quiescent clouds

Some suggested explanations of the second PLT

- Rotation of prestellar cores (Kritsuk et al. 2011), structures in rotationally flattened disks (Murray et al. 2017)
- Changing balance between gravity and turbulence in the course of MC evolution: first PLT signifies (Murray et al. 2017)
- Amplification of magnetic fields in the densest clumps within the cloud (Schneider et al. 2015)
- Change in thermodynamics: transition from isothermal state (at larger scales) to polytropic state (at small scales) in self-gravitating clouds with steady-state accretion (Donkov et al. 2021)

All those factors act together?

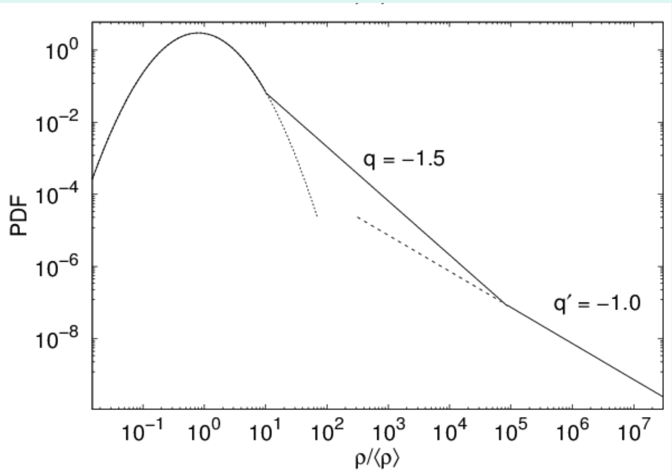

Some suggested explanations of the second PLT

- Rotation of prestellar cores (Kritsuk et al. 2011), structures in rotationally flattened disks (Murray et al. 2017)
- Changing balance between gravity and turbulence in the course of MC evolution: first PLT signifies (Murray et al. 2017)
- Amplification of magnetic fields in the densest clumps within the cloud (Schneider et al. 2015)
- Change in thermodynamics: transition from isothermal state (at larger scales) to polytropic state (at small scales) in self-gravitating clouds with steady-state accretion (Donkov et al. 2021)

All those factors act together?

This report: study of *ρ*-/*N*-PDF evolution which allows to distinguish the effect of rotation on the high-density end

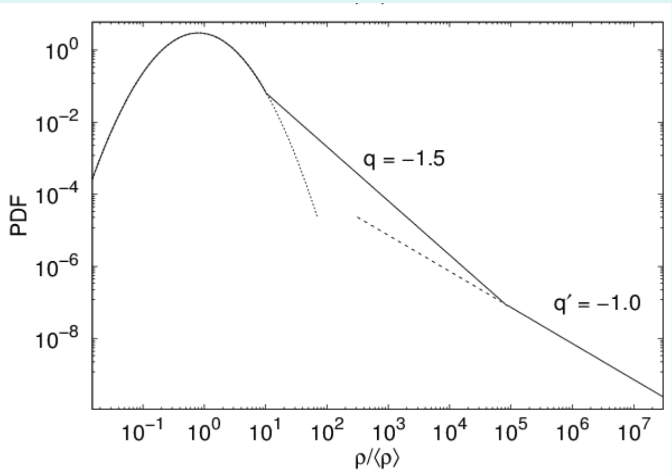

Used data and applied method

Numerical simulations (Wollenberg et al. 2020)

- Voronoi moving-mesh code AREPO (Springel 2010).
- Simulated contracting SF clump: single Bonnor-Ebert sphere within a homogeneous 13 pc box.
- Primordial gas: a network of 45 chemical reactions between different species of H and He and free electrons provides for treatment of cooling and for computation of the polytropic index
- Different physical setups
  - Pure infall (PI)
  - Rotation only (RO), β=0.01 and β=0.10
  - Turbulence only (TO), α=0.05 and α=0.25
- Run times: ~2 τ_{ff}; number of protostars formed: from 1 (PI) up to a few dozens

α Turbulent vs. gravitational potential energy ratio

β Rotational kinetic vs. gravitational potential energy ratio

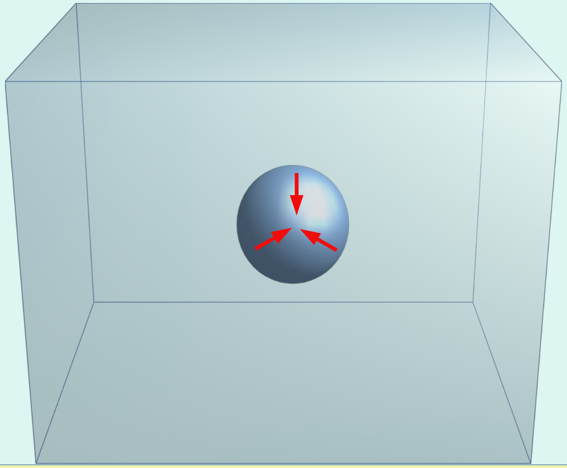

‘contracting SF clump’

BE-sphere: $R\sim2$ pc, $2.6\times10^{3}\,M_\odot$

Used data and applied method

Numerical simulations (Wollenberg et al. 2020)

- Voronoi moving-mesh code AREPO (Springel 2010).
- Simulated contracting SF clump: single Bonnor-Ebert sphere within a homogeneous 13 pc box.
- Primordial gas: a network of 45 chemical reactions between different species of H and He and free electrons provides for treatment of cooling and for computation of the polytropic index
- Different physical setups
  - Pure infall (PI)
  - Rotation only (RO), β=0.01 and β=0.10
  - Turbulence only (TO), α=0.05 and α=0.25
- Run times: ~2 τ_{ff}; number of protostars formed: from 1 (PI) up to a few dozens

α Turbulent vs. gravitational potential energy ratio

β Rotational kinetic vs. gravitational potential energy ratio

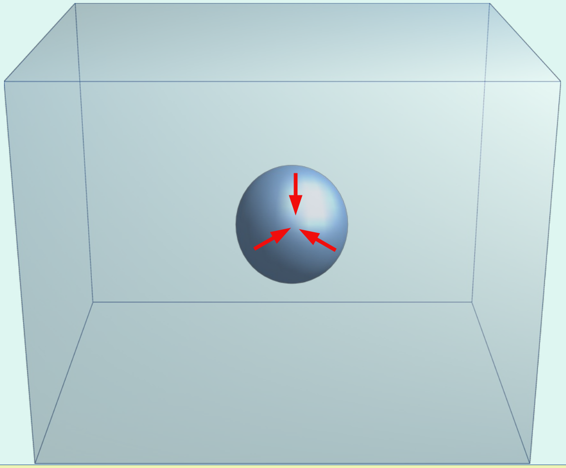

‘contracting SF clump’

BE-sphere: R~2 pc, 2.6x10^3 $M_\odot$

	Extension of the aBplfit technique (Veltchev et al. 2019)
	• Averaged PDFs (over varied total number of bins) • *Input parameters:* lower cutoff, upper cutoff, range of variation of the total number of bins. • *Output (PLT) parameters:* slope, deviation point

Development of multiple PLTs

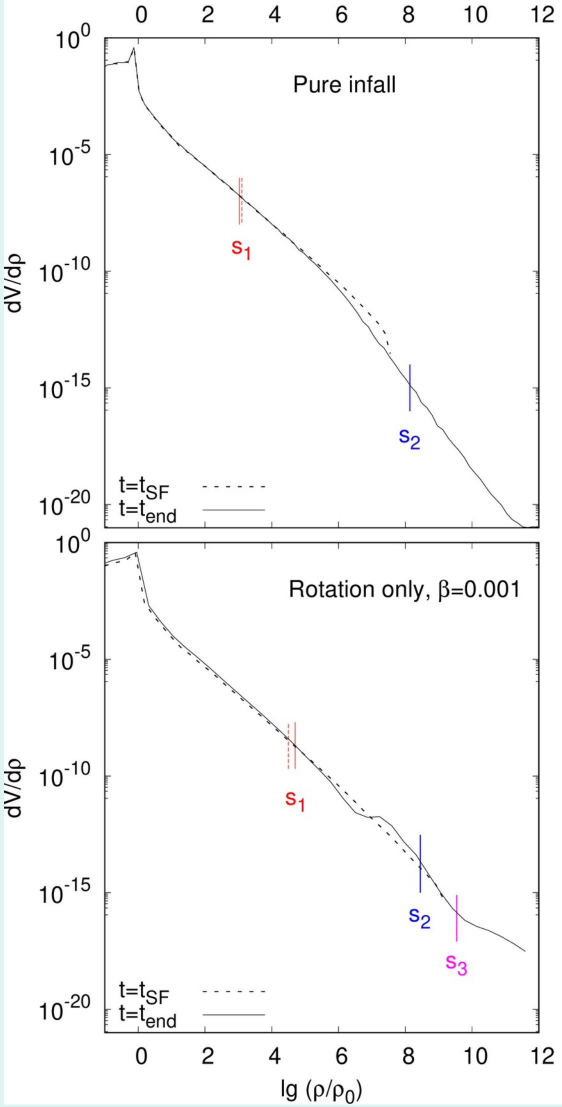

$t = t_{SF}$

$t = t_{end}$

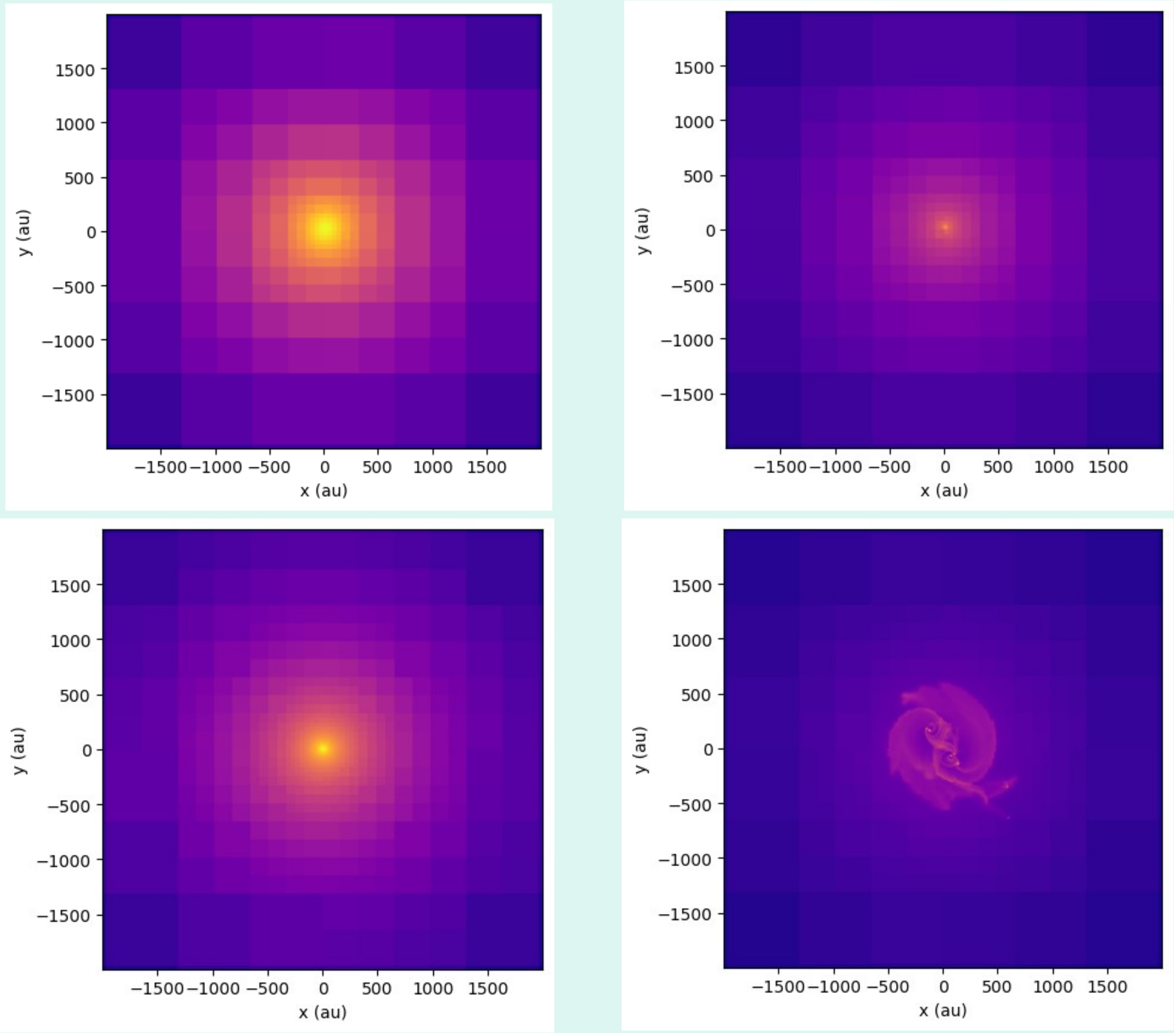

Evolution of the PLTs in ρ-PDFs

PI

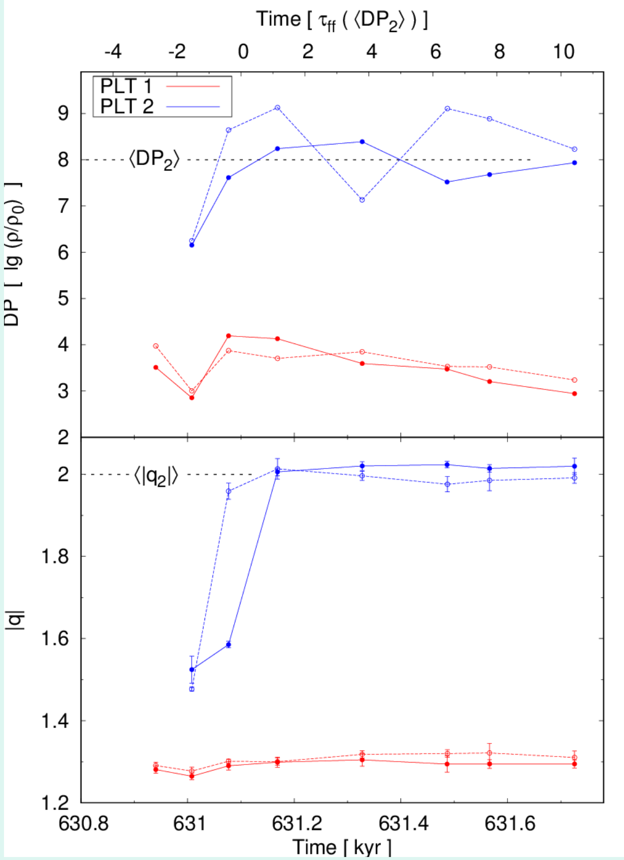

Evolution of the PLTs in ρ-PDFs

PI

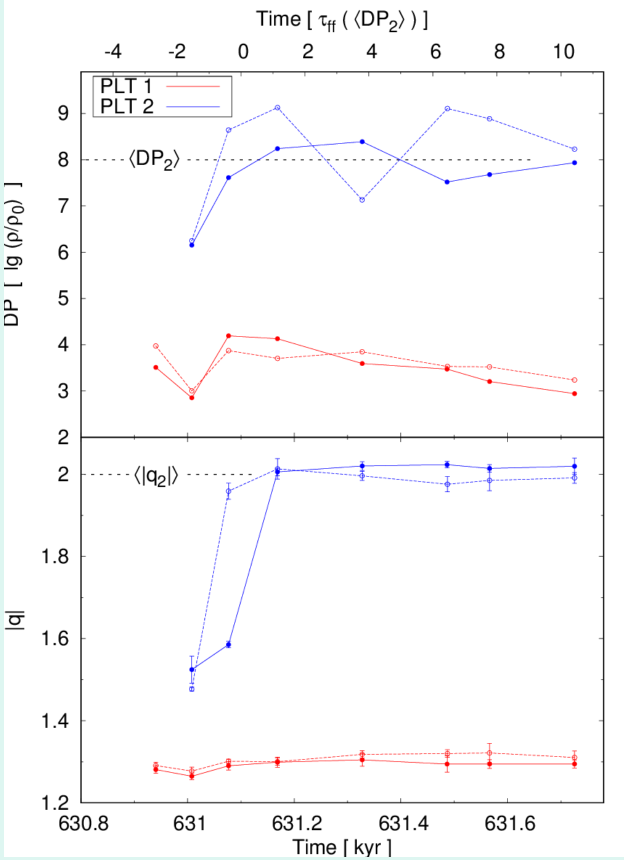

RO, β=0.01

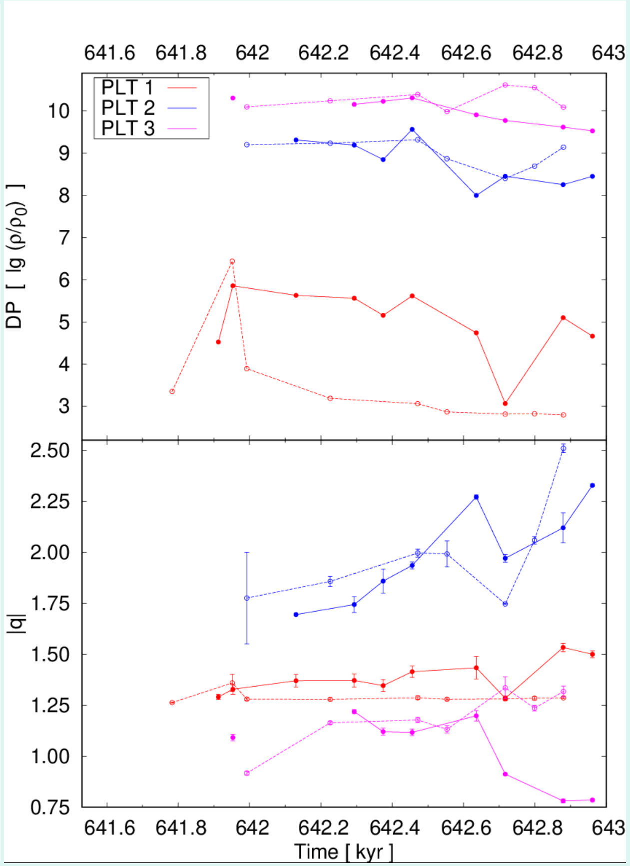

RO, β=0.10

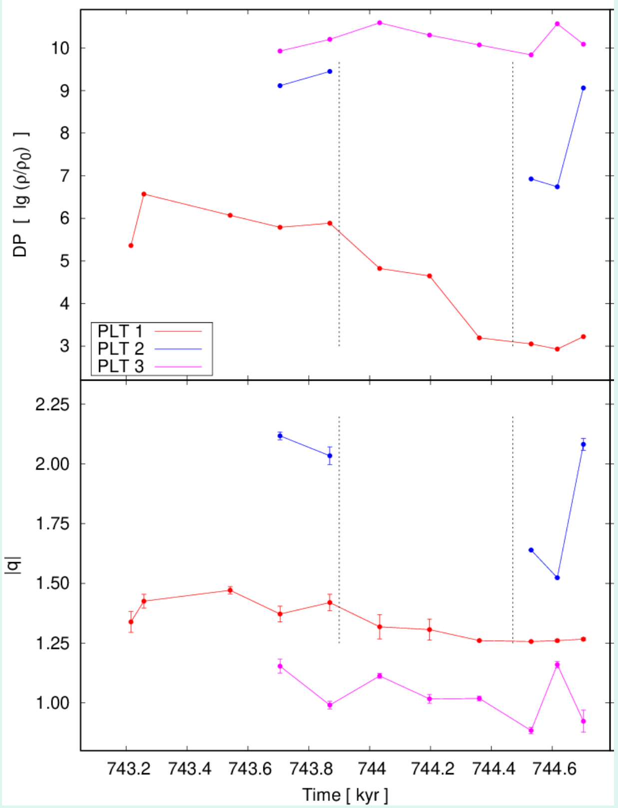

Evolution of the PLTs in *N*-PDFs

$$n = 2q/(3+q)$$

Donkov, Veltchev & Klessen (2017)

- Relation between the exponents of the PLTs in *ρ*– and *N*-PDF.
- Based on the assumption for spherical symmetry and density profile of power-law type.

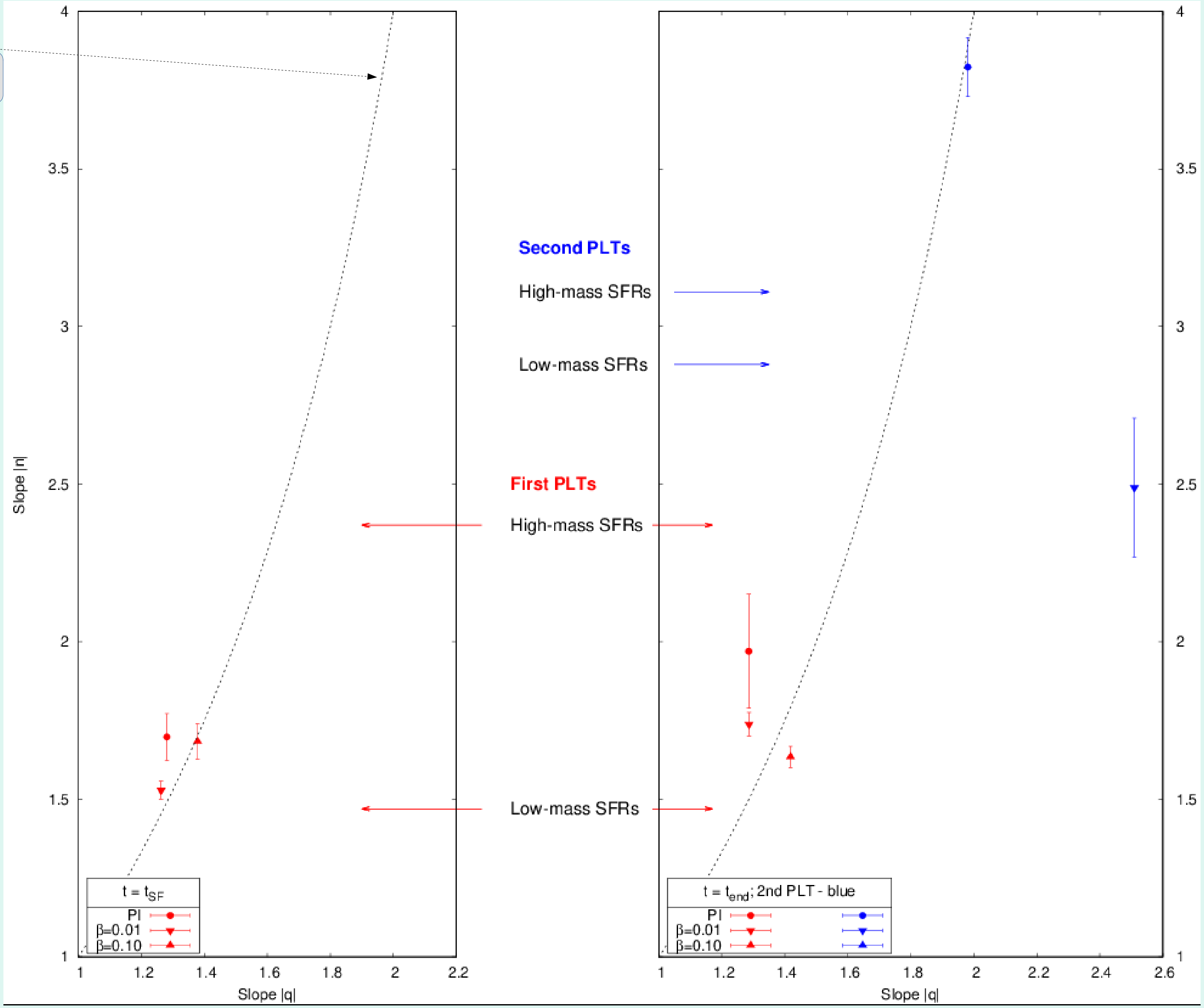

Evolution of the PLTs in *N*-PDFs

$$n = 2q/(3+q)$$

Donkov, Veltchev & Klessen (2017)

- Relation between the exponents of the PLTs in *ρ*– and *N*-PDF.
- Based on the assumption for spherical symmetry and density profile of power-law type.

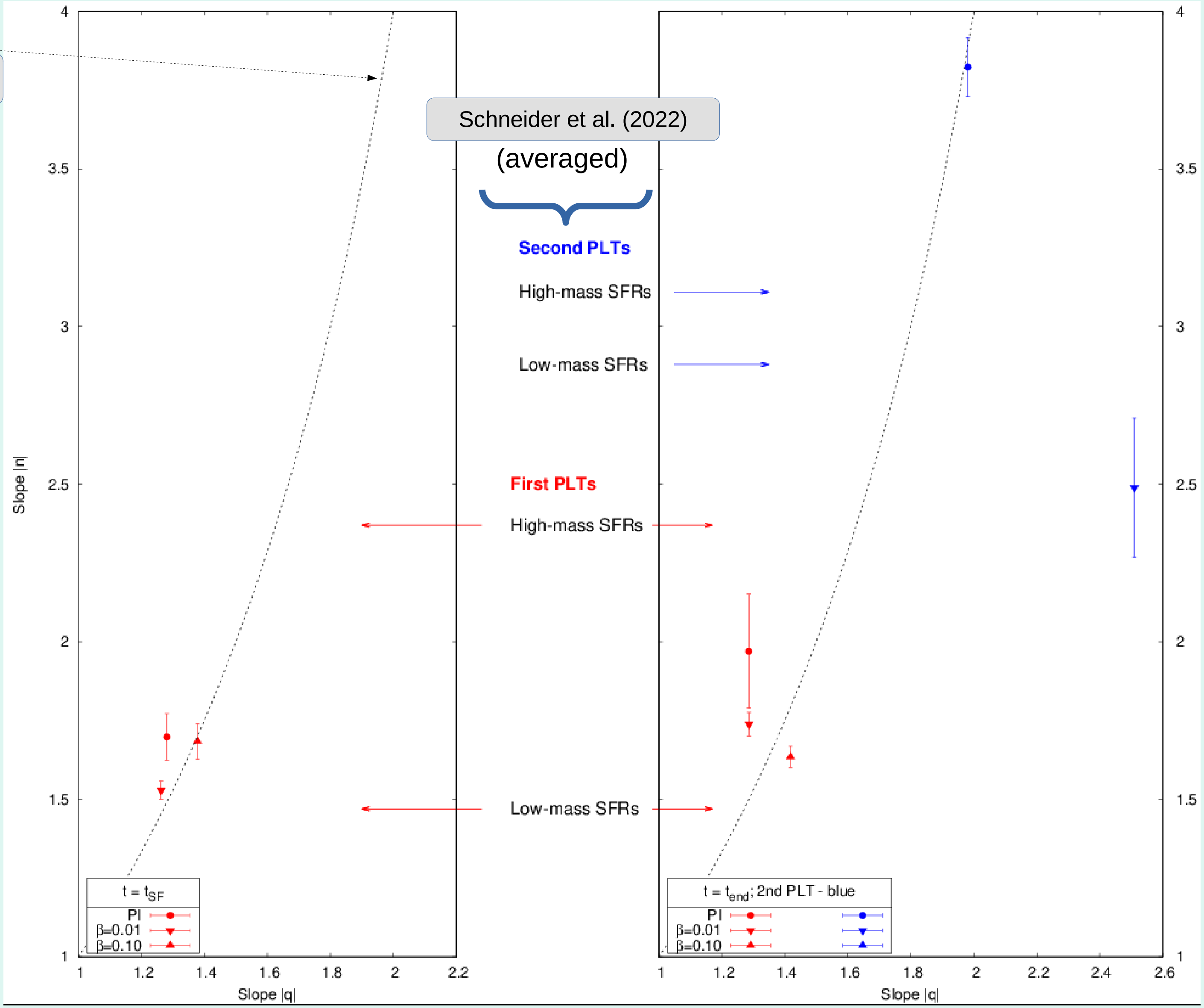

Schneider et al. (2022)

(averaged)

Second PLTs

High-mass SFRs

Low-mass SFRs

First PLTs

High-mass SFRs

Low-mass SFRs

Results: evolution of PLTs in SF clouds

- Similarities between all runs (pure infall and with rotational support)
  - Emergence of PLT 1 at $t \sim t_{SF}$; it retains its slope ($q_1 \sim -1.3$) within many free-fall times
  - Emergence (shortly after $t \sim t_{SF}$) and development of PLT 2 at the high-density end of the PDF, with a typical value $q_2 \sim -2.0$
  - *(For the runs with rotational support)* Emergence of PLT 3 at the very high-density end (i.e. very small spatial scales) whose slope varies around a typical value $q_3 \sim -1.0$
  - Relation between the PLT 1 slopes in ρ- and N-PDF corresponds to a spherically symmetric model with a radial PL density profile. They are in general agreement with the recent observations of regions of various SF activity (Schneider et al. 2022).
- Differences:
  - No PLT 3 in the pure-infall runs
  - Unstable PLT 2 in the RO runs; it disappears occasionally for β=0.10

Contribution: multiple PLTs in SF clouds/clumps

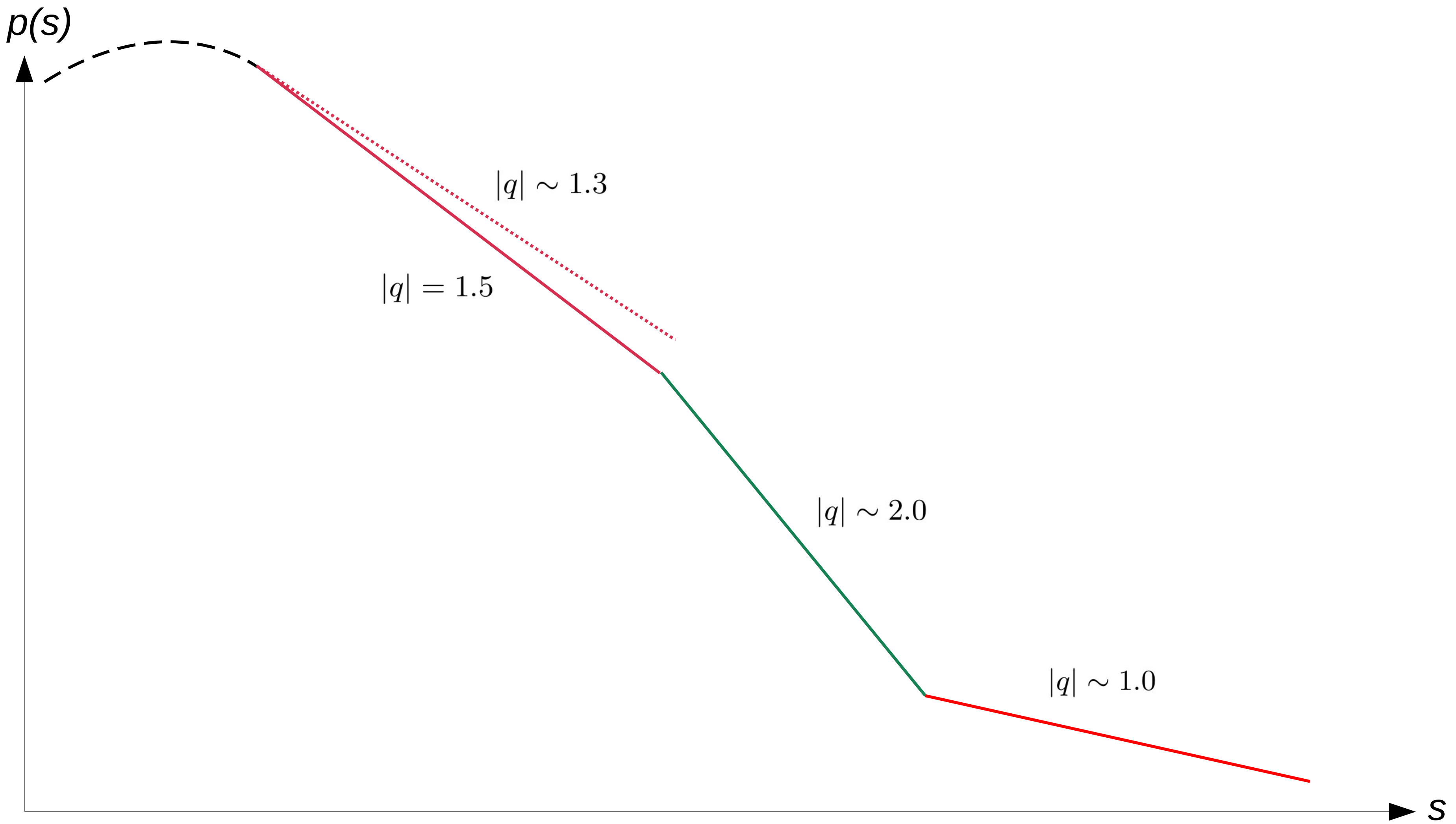

Contribution: multiple PLTs in SF clouds/clumps

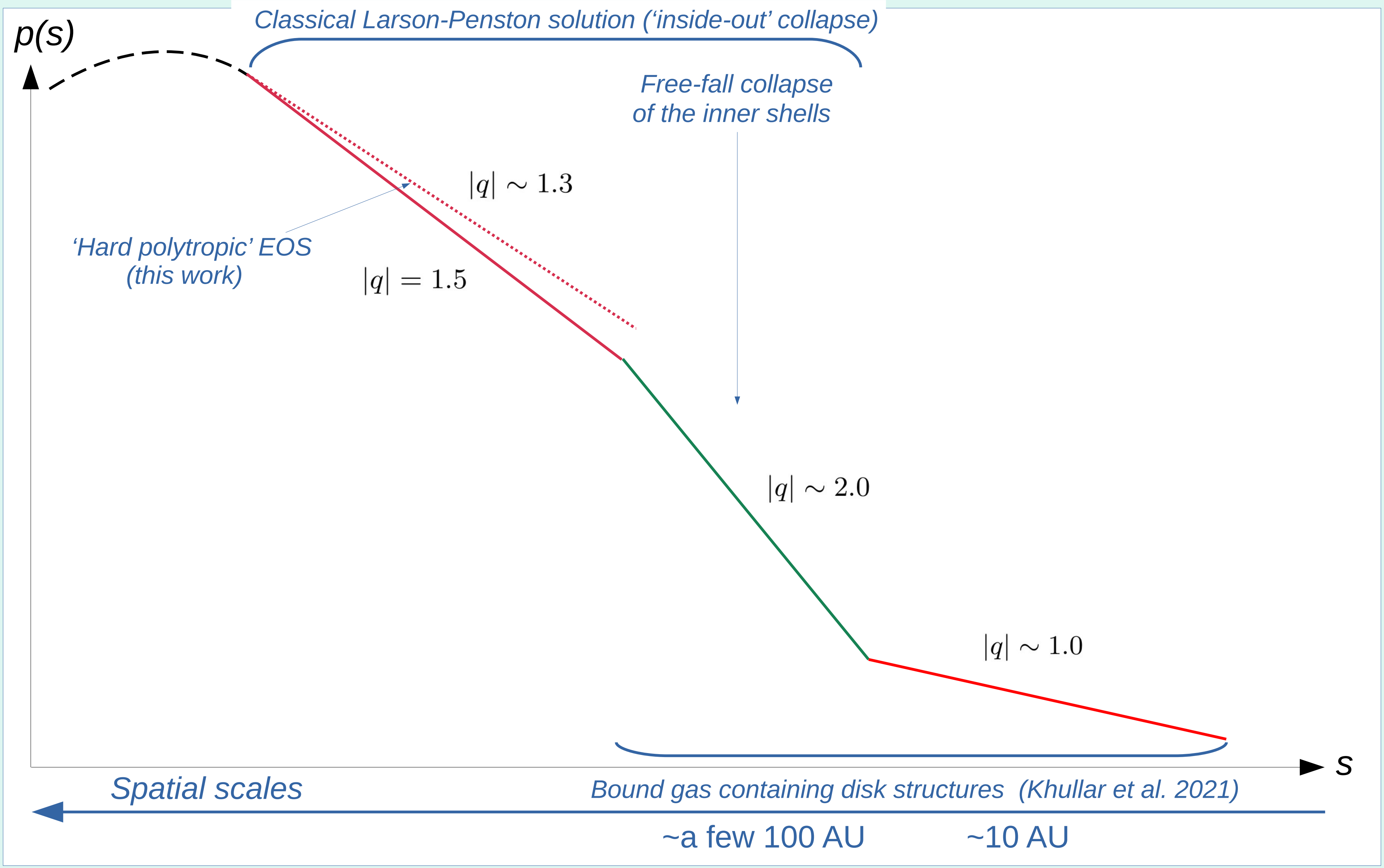

Contribution: multiple PLTs in SF clouds/clumps

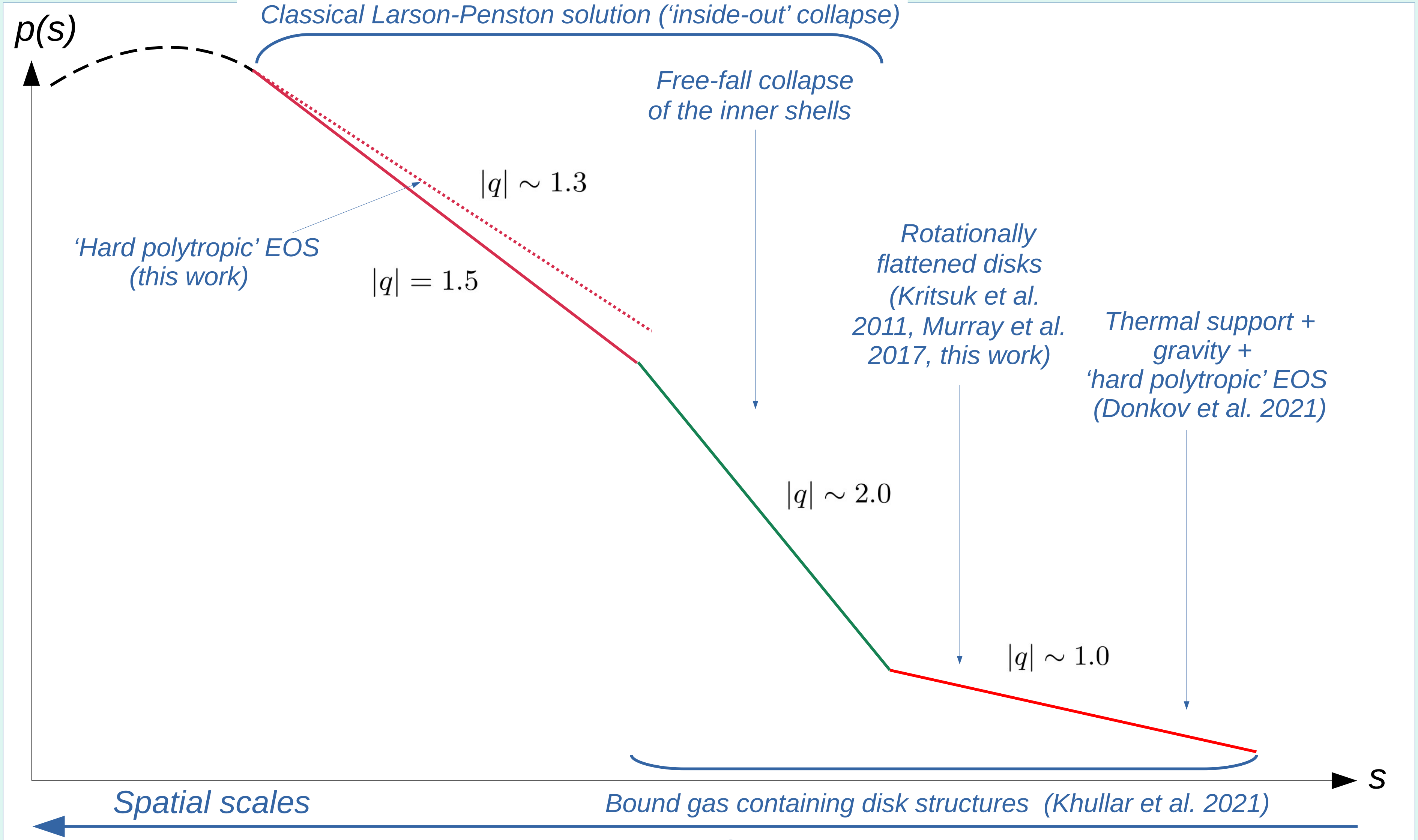

Acknowledgements

- Grant KL 1358/20- 3 of the Deutsche Forschungsgemeinschaft (DFG)
- Additional funding from the Ministry of Education and Science of the Republic of Bulgaria, National RI Roadmap Project DO1-176/29.07.2022